Environment International 138 (2020) 105588

Contents lists available at ScienceDirect

Environment International

journal homepage: www.elsevier.com/locate/envint

Energy efficiency of membrane distillation: Simplified analysis, heat recovery, and the use of waste-heat

Kofi S.S. Christie[a], Thomas Horseman[b], Shihong Lin[a,b,*]

[a] Department of Civil and Environmental Engineering, Vanderbilt University, Nashville, TN 37235, United States
[b] Department of Chemical and Biomolecular Engineering, Vanderbilt University, Nashville, TN 37235, United States

ARTICLE INFO

Handling Editor: Zhen (Jason) He

Keywords:
Membrane distillation
Energy efficiency
Module-scale analysis
Waste heat
Heat exchanger
Latent heat recovery

ABSTRACT

Membrane distillation (MD) is a thermal desalination process that is advantageous due to its ability to harness low-grade waste heat to separate highly saline feedstock. However, like any thermal desalination process, the energy efficiency depends on the ability to recover latent heat from condensation in the distillate. In direct contact MD (DCMD), this can be achieved by integrating a heat exchanger (HX) to recover latent heat stored in the distillate stream to preheat the incoming feed stream. Based on the principle of equal heat capacity flows, we derive a simple and intuitive expression for the optimal flow rate ratio between the feed and distillate streams to best recover this latent. Following the principle of energy balance, we derive simple expressions for the specific thermal energy consumption (SEC_{th}) and gained output ratio (GOR) of DCMD with and without a coupled HX for latent heat recovery, revealing an intuitive critical condition that indicates whether DCMD should or should not be coupled with HX. As MD is attractive for its ability to use low-grade waste heat as a heat source, we also evaluate the energy efficiency of DCMD powered by a waste heat stream. A waste heat stream differs fundamentally from a conventional constant-temperature heat source in that the temperature of the waste heat stream decreases as heat is extracted from it. We discuss the implication of this fundamental difference on energy efficiency and how we should analyze the energy efficiency of DCMD powered by waste heat streams. A new metric, namely specific yield, is proposed to quantify the performance of DCMD powered by waste heat stream. Our analysis suggests that, for a single-stage DCMD powered by a waste heat stream, whether implementing latent heat recovery or not only affects conventional metrics for energy efficiency (e.g. SEC_{th} and GOR) but not the specific yield. Overall, this analysis presents an intuitive and important framework for evaluating and optimizing energy efficiency in DCMD.

1. Introduction

Membrane distillation (MD) is a thermally-driven liquid separation process which shows promise for desalination and the treatment of highly saline wastewater. (Shaffer, 2013; Deshmukh, 2018; Alkhudhiri et al., 2012) In direct contact MD (DCMD), a microporous and hydrophobic membrane is used to separate a heated feed solution and a cool distillate solution. Water vapor passes across the MD membrane from the feed solution to the distillate solution due to a partial vapor pressure difference between the two streams. Unlike reverse osmosis in which the applied pressure must exceed the brine osmotic pressure and thus become unpractical with high-salinity feed solution, the applicability of MD is less sensitive to feed salinity due to the relatively weak dependence of partial vapor pressure on salinity. This advantage, along with the fact that MD can be operated using low-grade waste heat, contribute to the interest in MD for desalination, hypersaline brine management, and zero liquid discharge. (Curcio and Drioli, 2005; Drioli et al., 2015; Camacho, 2013; Creusen, 2013; Tong and Elimelech, 2016; Semblante et al., 2018)

As water vapor crosses the membrane in MD, the transfer of heat and mass are fundamentally connected. The mass transfer rate across the membrane is driven by the membrane permeability and the partial vapor pressure gradient, which is predominantly a function of temperature. Heat is transferred across the membrane with the vapor via convection, where the rate is governed by the vapor flux, and via conduction through the vapor-membrane system, where the rate is a function of the system's thermal conductivity. An abundance of literature has been presented on the investigation of simultaneous heat and mass transfer across the MD boundary layers. (Alklaibi and Lior, 2006; Schofield et al., 1987; Qtaishat et al., 2008; Termpiyakul et al., 2005; Phattaranawik and Jiraratananon, 2001; Gryta and Tomaszewska, 1998; Phattaranawik et al., 2003) They often involve the resolution of

* Corresponding author at: Department of Civil and Environmental Engineering, Vanderbilt University, Nashville TN 37235, United States.
E-mail address: shihong.lin@vanderbilt.edu (S. Lin).

https://doi.org/10.1016/j.envint.2020.105588
Received 24 November 2019; Received in revised form 15 February 2020; Accepted 16 February 2020
Available online 29 February 2020

Nomenclature

α	flow rate ratio (i.e., the ratio between the distillate flow rate and feed flow rate) [Dimensionless]
α^*	critical flow rate ratio [Dimensionless]
η_{th}	thermal efficiency, i.e., the percentage of *trans*-membrane heat transfer that is contributed by the transfer of latent heat [Dimensionless]
η_{ws}	waste-heat utilization efficiency [Dimensionless]
$\eta_{ws,k}$	waste-heat utilization efficiency for the kth stage [Dimensionless]
c_F	specific heat capacity of the feed solution [kJ kg^{-1} °C^{-1}]
c_D	specific heat capacity of the distillate [kJ kg^{-1} °C^{-1}]
c_{ws}	specific heat capacity of the waste heat stream [kJ kg^{-1} °C^{-1}]
GOR	gained output ratio [Dimensionless]
$\bar{h}_{vap}$	enthalpy of vaporization (i.e., latent heat) [kJ kg^{-1}]
P_{th}	(thermal) power of heat absorbed in the heat source [kW]
$P_{th,max,ws}$	(thermal) power of the available heat in the waste heat stream [kW]
Q_D	distillate flow rate [kg min^{-1}]
Q_F	feed flow rate [kg min^{-1}]
Q_{ws}	flow rate of the waste heat stream [kg min^{-1}]
ΔQ	change of either feed or distillate stream flow rate (they are the same), which is also the cross-membrane vapor flow rate [kg min^{-1}]
ΔQ_{max}	maximum cross-membrane vapor flow rate [kg min^{-1}]
R	water recovery in a single pass [Dimensionless]
R_{max}	maximum water recovery in a single pass [Dimensionless]
R_{max}^{DLR}	maximum water recovery in a single pass when the system is in distillate limited regime [Dimensionless]
R_{max}^{FLR}	maximum water recovery in a single pass when the system is in feed limited regime [Dimensionless]
SEC_{th}	specific thermal energy consumption, i.e., energy consumed to generate a unit mass of distillate [kJ kg^{-1}]
$SEC_{th,k}$	specific thermal energy consumption for the kth stage [kJ kg^{-1}]
SY	specific yield [Kg min^{-1} kW^{-1}]
ΔT	temperature difference between the influent temperatures of the feed and distillate streams (i.e., $T_H - T_C$) [°C]
	influent temperature of the distillate stream [°C]
T_H	influent temperature of the feed stream [°C]
ΔT_{HS}	temperature gain of the feed stream after going through the heat source ($=T_H - T_{mix}$) [°C]
ΔT_{HX}	temperature difference between the hot and cold streams in the HX [°C]
ΔT_{MD}	trans-membrane difference in the DCMD module [°C]
T_{mix}	temperature of the stream obtained from mixing the feed water and the effluent of the MD feed stream [°C]
$T_{ws,i}$	influent temperature of the waste heat stream [°C]
$T_{ws,e}$	effluent temperature of the waste heat stream [°C]

large systems of coupled equations for which the results give accurate predictions of how varying membrane properties and operating conditions affect the transmembrane vapor flux. These studies have even been confirmed in benchtop experiments with membrane coupons (Termpiyakul et al., 2005; Gryta and Tomaszewska, 1998; Martínez-Díez et al., 1998; Martínez-Díez and Vázquez-González, 2000; Phattaranawik et al., 2001; Cath et al., 2004).

The rigorous heat and mass transfer modelling in the aforementioned studies does not readily extend to an analysis of overall energy expenditure in MD, especially on the module scale. While studies have compared the energy efficiency of common MD configurations (Swaminathan et al., 2016; Swaminathan, 2016), module scale analysis is important because industrial application of MD requires much larger membrane surface areas and the effect of the temperature drop along the module is typically overlooked. (Song et al., 2007; Cheng et al., 2008; Bui et al., 2010; Zuo et al., 2011; Summers et al., 2012; Swaminathan et al., 2016) Module scale modelling is also important because energy consumption in MD typically exceeds that of other non-thermal desalination processes, (Summers et al., 2012; Warsinger et al., 2015; Shannon, 2009) so industrial application of MD hinges upon successful measures of latent heat recovery. Previous studies that have explored the MD-HX system (Lee et al., 2011; Hausmann et al., 2012; Maheswari et al., 2015; Kim et al., 2015; Lu and Chen, 2012; González-Bravo et al., 2015; Chung et al., 2014; Guan et al., 2015; Gustafson et al., 2018) lack the simplicity required to build an intuitive understanding of the tradeoffs and opportunities inherent within the typical range of operation. Further, the clarity surrounding the discussion of heat energy utilization and process efficiency can be improved. That is, the grand scheme regarding how energy efficiency should be analyzed is still missing.

In this work, we present a module-scale thermodynamic analysis to explore the energy efficiency of direct contact membrane distillation (DCMD) through the introduction of simplified thermodynamic criteria for MD design and operation. We evaluate energy consumption in MD with and without a coupled HX system to recover latent heat from condensation in the distillate stream. We also consider the energy efficiency and waste-heat source energy utilization efficiency when operating MD with and without coupled HX for latent heat recovery with a waste-heat stream as the heat source (as theorized for industrial application). We apply reasonable simplifying assumptions to the MD process to demonstrate how the key parameters in MD behave on the module scale. Our analysis establishes a framework for evaluating the thermodynamic efficiency of the MD process and facilitates an intuitive understanding of how operational and configurational decisions affect the energy efficiency of MD.

2. Simplified thermodynamic criteria for MD design and operation

Before performing energy efficiency analysis for an MD system, we would like to first re-visit the basic criteria for optimizing design and operation of a module-scale DCMD system and system's performance limit based on thermodynamics. While these principles have been presented before in more rigorous forms, the goal of the discussion here is to simplify the governing equations of these principles to impart an intuitive understanding with minimal loss of accuracy.

2.1. Flow balancing rule

It is convenient to use an equal flow rate for both the feed and distillate streams, in which case the flow rate ratio, α (i.e., the ratio of the distillate to the feed flow rate, Q_D/Q_F) is simply unity. However, recent studies have found that $\alpha = 1$ is generally not an optimal operating condition. (Swaminathan et al., 2016; Lin et al., 2014) Because the feed salinity is typically very high in the context of MD, the specific heat capacity of the feed stream, c_F, is substantially lower than that of the distillate stream, c_D. If the same flow rate, Q, is used for both streams, the heat capacity flow (i.e., heat capacity per time) of the feed stream, as quantified by Qc_F, is substantially lower than that of the distillate stream as quantified by Qc_D. This unbalance in heat capacity flow between the two streams will lead to sub-optimal system performance in terms of membrane utilization and energy efficiency. (Swaminathan et al., 2016; Lin et al., 2014; Bergman et al., 2011)

The critical flow rate ratio, α^*, for a DCMD process with counter-current flows has been previously derived via thermodynamic analysis of a DCMD module. (Lin et al., 2014) This critical flow rate ratio represents the condition in which the operation is optimal. However, the

expression for α^* is complicated and involves functions that have to be evaluated numerically. Following the principle of balancing heat capacity flow (i.e., $Q_F c_F = Q_D c_D$), (Bergman et al., 2011) a simple approximation of α^* is the ratio between the specific heat capacities of feed stream, c_F, and that of the distillate stream, c_D (i.e., $\alpha^* = c_F/c_D$). Such a simple approximation of α^* can deviate from the exact α^* to a substantial extent (Fig. 1A), primarily due to the changes of flow rates in the DCMD module as water recovery reduces the feed flow rate and increases the distillate flow rate.

Here, we present an alternative approximation of α^* that does not involve any function requiring numerical evaluation. This approximation is obtained based on equation 37 of reference 40 (Lin et al., 2014) by removing or adjusting terms that are not intrinsic properties of the solution and cannot be directly determined. The alternative approximation is given as

$$\alpha^* = \frac{c_F}{c_D}\frac{\bar{h}_{vap} - c_F \Delta T/2}{\bar{h}_{vap} + c_D \Delta T/2} = \frac{c_F}{c_D}\varphi(\bar{h}_{vap}, c_D, c_F, \Delta T) \quad (1)$$

where $\bar{h}_{vap}$ is the average enthalpy of vaporization of water and ΔT is the difference between the influent temperature of the saline feed stream (T_H) and that of the distillate stream (T_C). Because $\bar{h}_{vap}$ is slightly dependent on temperature, its value can be evaluated using the average temperature of T_H and T_C. We note that enthalpy of vaporization only has very weak dependence on salinity and we therefore use the h_v for pure water throughout our discussion in this paper. Eq. (1) is derived simply by ignoring the "threshold temperature difference" (SI Section 2). This equation of α^* differs from $\alpha^* = c_F/c_D$ by a correction factor, $\varphi(\bar{h}_{vap}, c_D, c_F, \Delta T)$, that is always higher than unity. This correction factor roughly accounts for the change of the heat capacity flows of both the feed and distillate streams due to the decrease of the feed stream flow rate and increase of the distillate stream flow rate during the DCMD operation. This modified expression (Eq. (1)), simple and without obscure functions, can provide an outstanding approximation of the exact α^* (Fig. 1B).

2.2. Thermodynamic limit of single-pass water recovery

Another important observation from module-scale thermodynamic analysis is the presence of the limit for a single-pass water recovery, R_{max} . The presence of this limit can be explained by a relatively simple principle. When there is sufficient membrane area to allow for the greatest extent of heat and vapor transport possible, there are two possible scenarios. In scenario (1) called distillate limiting regime (DLR, where $\alpha < \alpha^*$), the distillate water is limited as compared to the feed water. In this case, when a fraction of the feed water evaporates, the evaporation transfers sufficient amount of latent heat to warm up the distillate stream to an extent that the driving force for vapor transport (i.e., the partial vapor pressure difference) vanishes (Fig. 2A). In scenario (2) called feed limiting regime (FLR) where $\alpha > \alpha^*$, when a sufficient fraction of the feed water evaporates, the evaporation carries away a large amount of latent heat and thereby cools down the feed stream to an extent that the driving force for vapor transport vanishes (Fig. 2B). In both cases, this fraction represents the limit for single-pass water recovery as it is thermodynamically infeasible to recover a fraction of the feed water larger than this theoretical limit in a single-pass.

Here we derive simple and intuitive approximations of the limits of the single-pass recovery in both the DLR and FLR, considering the impact of the conductive heat transfer as quantified by thermal efficiency, η_{th}. Briefly, η_{th} is the ratio of the amount of heat transferred via vapor transport over the total amount of heat transferred via both vapor transport and thermal conduction. In the DLR, the distillate temperature will increase by approximately ΔT, i.e., from T_C to T_H, if we neglect the threshold temperature difference. Therefore, the heat gained by the distillate stream is roughly $Q_D c_D \Delta T$, if we do not consider the minor change in the distillate flow rate. Only part of this heat gain, which is $\eta_{th} Q_D c_D \Delta T$, is from the latent heat of condensation. If the mass of the vapor transferred across the membrane is ΔQ, the latent heat of condensation is roughly $\Delta Q \bar{h}_{vap}$. When membrane area is sufficient, ΔQ reaches its maximum ΔQ_{max}, which can be described using the following equation based on energy balance and the definition of flow rate ratio α (Q_D/Q_F).

$$\eta_{th} \alpha Q_F c_D \Delta T = \Delta Q_{max} \bar{h}_{vap} \quad (2)$$

Based on these relationships, we arrive in the approximate expression for the theoretical maximum recovery (assuming sufficient membrane area) for DLR:

$$R_{max}^{DLR} = \frac{\Delta Q_{max}}{Q_F} = \frac{\eta_{th} c_D}{\bar{h}_{vap}} \alpha \Delta T \quad (3)$$

Following a similar logic, the feed temperature will decrease by approximately ΔT, i.e., from T_H to T_C, when the system is in a FLR with sufficient membrane area and $\alpha > \alpha^*$. In this case, the heat loss in the feed stream is roughly $Q_F c_F \Delta T$, if we do not consider the minor change in the feed flow rate. Part of this heat loss, roughly $\eta_{th} Q_F c_F \Delta T$, provides the latent heat for evaporation which is approximately $\Delta Q \bar{h}_{vap}$. With sufficient membrane area, ΔQ reaches its maximum ΔQ_{max}, which leads to the following energy balance equation:

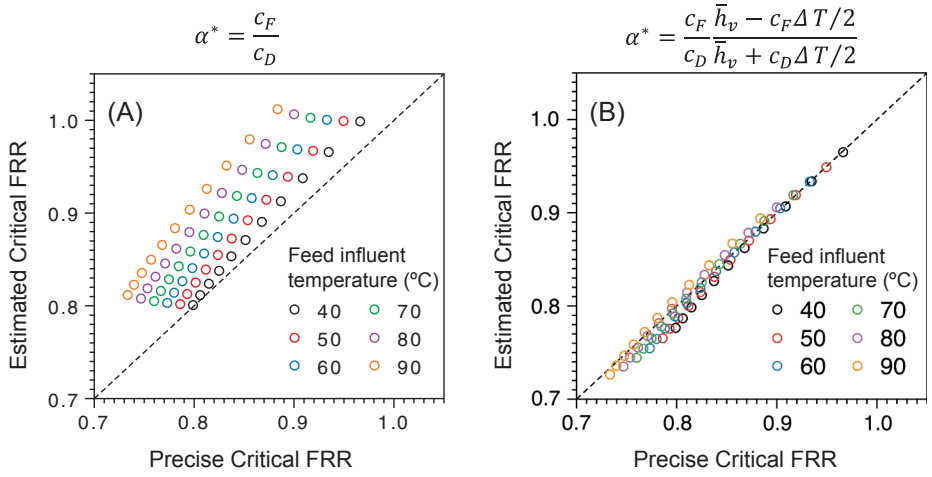

Fig. 1. Estimated critical flow rate ratio (FRR, α*) vs. precise critical FRR as given by Eq. S1. The estimated α^* is calculated using the approximate equation given on the top of each panel. In each panel, six feed influent temperatures, T_H, are used in the simulation. In each series, the molality of the feed solution ranges from 0 to 5 mol kg^{-1} (of water). The distillate temperature is fixed at 20 °C. The molality of the distillate is assumed to be zero.

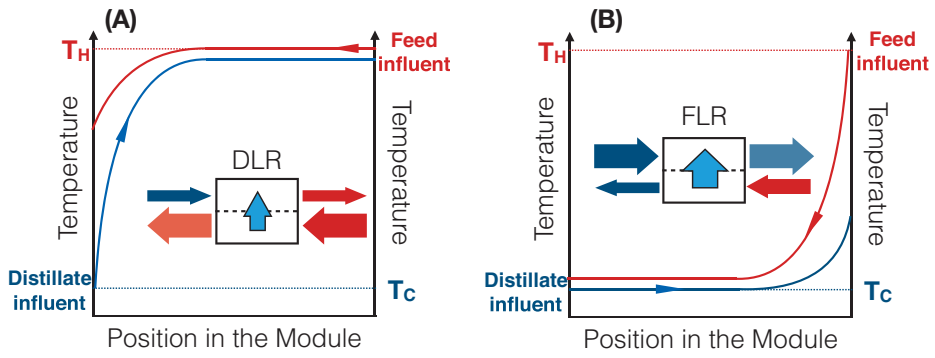

Fig. 2. Schematic illustrations of (A) distillate limiting regime (DLR) and (B) feed limiting regime (FLR) in a DCMD module. In DLR, the distillate flow rate is small compared to the feed flow rate, so that the distillate temperature rises up in the module to approach the feed influent temperature. In FLR, the feed flow rate is small compared to the distillate flow rate, so that the feed temperature drops in the module to approach the distillate influent temperature. In both cases, the difference in salinity of the two streams leads to a small temperature difference when the driving force (i.e., partial vapor pressure difference between the two streams) vanishes to zero.

$$\eta_{th} Q_F c_F \Delta T = \Delta Q_{max} \bar{h}_{vap} \tag{4}$$

The approximate expression for the theoretical maximum recovery (assuming sufficient membrane area) in FLR is then given by

$$R_{max}^{FLR} = \frac{\Delta Q_{max}}{Q_F} = \frac{\eta_{th} c_F}{\bar{h}_{vap}} \Delta T \tag{5}$$

Combining Eq. (3)–(5), suggest that R_{max}^{FLR} is always higher than R_{max}^{DLR}, which is reasonable because only in FLR does the distillate stream have enough heat capacity flow to ensure that the maximum evaporation of the feed stream can be achieved. Therefore, R_{max}^{FLR} is the ultimate limit for single-pass water recovery for counter-current flow DCMD.

Even though derived with a few simplifying assumptions, Eq. (5) provides a remarkable approximation of the maximum single-pass water recovery predicted from more detailed and accurate analysis reported in the previous work (Fig. 3). (Lin et al., 2014) In an ideal scenario with perfect thermal efficiency, R_{max} simply becomes $c_F \Delta T / \bar{h}_{vap}$. For seawater, $c_F / \bar{h}_v$ is roughly 1/600 K^{-1}. Therefore, even with a temperature difference ΔT of 60 K, the theoretical maximum single-pass recovery is only 10%. With the finite membrane area and realistic thermal efficiency, η_{th}, the realistic single pass-recovery can be significantly lower. Readers with interest in the impacts of system size and thermal efficiency can refer to the recent work by Swaminathan et al (Swaminathan et al., 2018).

3. Energy efficiency analysis for MD driven by conventional heat source

In this section we present a simple framework to analyze the energy efficiency of a DCMD system powered by conventional heat source with and without a heat exchanger (HX). A conventional heat source is defined as a heat source with a constant temperature. Its function is to increase the temperature of the feed stream to T_H by providing the required amount of (thermal) power, P_{th}. In comparison, when a stream containing waste-heat is used as the heat source, the temperature of the heat source decreases as more heat is extracted. Whether the temperature of the heat source changes when it transfers thermal energy to the feed stream in MD is the primary difference between a conventional heat source and a stream with waste-heat as the heat source.

We have shown in Section 2.2 that only a small fraction of the feed water can be recovered in a single pass. Because feed water needs to be pretreated and is thus associated with certain cost, recycling of the feed stream effluent is likely practiced in most practical operation. When the feed stream is recycled, a stream of feed water with the same flow rate as the *trans*-membrane flow rate, ΔQ, should be supplemented to the feed loop to maintain steady-state of the flows (Fig. 4A, Fig. 5A). The same flow rate ΔQ is also extracted from the distillate loop. We note that even though steady-state for the flows can be achieved, the system still behaves transiently due to the accumulation of the salt in the feed loop. There are two different designs for a counter-current DCMD system with recycled feed and distillate streams. The primary difference is that an HX is not implemented in the first design (Fig. 4A) but implemented for heat recovery in the second design (Fig. 5A).

It is reasonable to assume that the temperature differences across the membrane in the DCMD module and across the HX are both spatially uniform along the module and HX, respectively, as long as the membrane area and the size of the HX are not impractically large and the flow rates are optimized based on the critical flow rate ratio. This assumption of constant temperature difference, which is reasonable based on pervious simulations, highly simplifies the following analysis. Here, we are not interested in developing or applying a predictive model to describe system performance. Instead, we aim to develop a simple framework for quantifying energy efficiency provided that we know the *trans*-membrane temperature difference in the MD system, ΔT_{MD}, the temperature difference in the HX, ΔT_{HX}, the working temperatures T_H and T_C, and finally, the thermal efficiency, η_{th}.

3.1. Specific energy consumption for a DCMD system without HX

If the *trans*-membrane temperature difference is ΔT_{MD} throughout the MD module, the effluent feed temperature is ΔT_{MD} higher than the influent temperature of the distillate and is thus $T_C + \Delta T_{MD}$. In the absence of HX, the effluent of the feed stream with a flow rate of $Q_F - \Delta Q$ is blended with the supplementing new feed stream with a flow rate of ΔQ (Fig. 4A). This blending reduces the temperature of the feed effluent by a small degree. The temperature of the blended stream, T_{mix}, can be calculated based on energy balance:

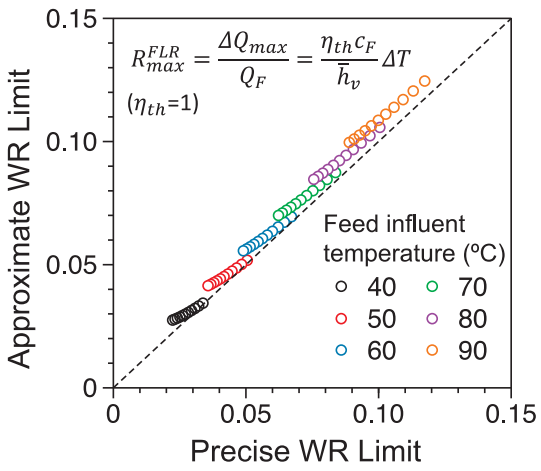

Fig. 3. Estimated maximum single pass water recovery (WR, R_{max}^{FLR}) versus the precise WR given by **Eq. S6**. The estimated R_{max}^{FLR} is calculated using the equation given in the top of the figure assuming ideal thermal efficiency (η_{th} = 1). Six feed influent temperatures, T_H, are used in the simulation. In each series, the molality of the feed solution ranges from 0 to 5 mol kg^{-1} (of water). The distillate temperature is fixed at 20 °C. The molality of the distillate is assumed to be zero.

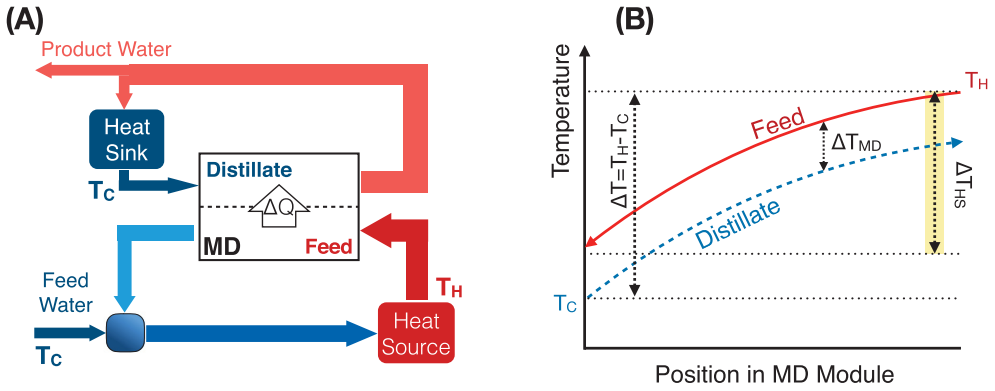

Fig. 4. (A) Countercurrent DCMD system with recycled feed and distillate streams in the absence of HX to recover latent heat from the distillate stream. A heat source is required to maintain the working temperature (T_H) and a heat sink is required to maintain the distillate inlet temperature (T_C). (B) Temperature profiles of the feed and distillate streams along the module in (A). The DCMD feed inlet temperature, initially at T_H, drops along the module due to evaporative cooling and conduction, reaching $T_C + \Delta T_{MD}$ at the feed outlet. The transmembrane vapor flux, ΔQ, is added to supplement the feed stream (at T_C) to maintain constant flow rate ratio, bringing the feed loop temperature down very slightly to T_{mix}. Before returning to the feed inlet, the feed passes a heat source where it undergoes the temperature change ΔT_{HS}, which is related to the power input into the system. The distillate inlet temperature, initially at T_C, increases along the module due to vapor condensation and conduction, reaching $T_H - \Delta T_{MD}$ at the distillate outlet. The transmembrane vapor flux, ΔQ, is removed from the system to maintain constant flow rate ratio and the remaining distillate passes a heat sink where it reaches the operating temperature, T_C.

$$T_{mix} = T_C + (1 - R)\Delta T_{MD} \tag{6}$$

where R is the single-pass water recovery which is usually negligibly small. To further simplify our analysis, we ignore R and treat T_{mix} as $T_C + \Delta T_{MD}$, which would lead to slight underestimation of the energy consumption but much simpler expressions.

In the absence of an HX, the feed stream after blending needs to go through the heat source so that its temperature is raised to the working temperature T_H (Fig. 4B). The temperature gain of the feed stream in the heat source, ΔT_{HS}, is given by

$$\Delta T_{HS} = T_H - T_{mix} \approx T_H - T_C - \Delta T_{MD} = \Delta T - \Delta T_{MD} \tag{7}$$

Therefore, the thermal power of heat absorbed in the heat source, P_{th}, is simply

$$P_{th} = c_F Q_F \Delta T_{HS} \tag{8}$$

After quantifying the power of heat input from the heat source, we also need to evaluate the product water flow rate which is essentially the transmembrane flow rate, ΔQ (Fig. 4A). This can be performed using similar energy balance approach as shown in Section 2.2. Specifically, the temperature drop along the feed stream is $\Delta T - \Delta T_{MD}$ and the heat lost along the feed stream is roughly $c_F Q_F(\Delta T - \Delta T_{MD})$. The *trans*-membrane flow rate can therefore be expressed as

$$\Delta Q = \frac{c_F Q_F(\Delta T - \Delta T_{MD})\eta_{th}}{\bar{h}_{vap}} \tag{9}$$

The energy efficiency of the process can be quantified using the specific thermal energy consumption, SEC_{th}, defined as the energy consumed to generate a unit mass of distillate which is essentially the power required to generate a unit flow rate of distillate:

$$SEC_{th} = \frac{P_{th}}{\Delta Q} = \frac{\bar{h}_{vap}}{\eta_{th}} \tag{10}$$

Eq. (10) is rather intuitive as η_{th} quantifies the fraction of the heat transfer that is attributable to vapor transfer. According to Eq. (10), DCMD without HX can be even more energy intensive than just evaporating water due to the presence of conductive heat loss. While c_F appears in both Eq. (8) and (9), it cancels out in Eq. (10), which has the following important implication. Although the salt concentration in the feed loop increases as more water is recovered from the feed solution, the build-up of salt concentration theoretically has little impact on SEC_{th} because (1) the significant impact of salt concentration on c_F applies equally to both P_{th} and ΔQ which offset each other, and (2) the

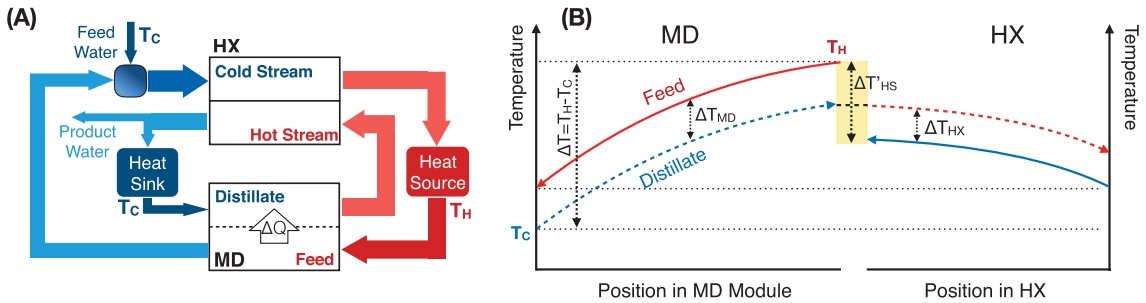

Fig. 5. (A) Countercurrent DCMD system with recycled feed and distillate streams and an HX to recover latent heat from the distillate stream. A heat source is required to maintain the working temperature (T_H) and a heat sink is required to maintain the distillate inlet temperature (T_C). (B) Temperature profiles of the feed and distillate streams along the DCMD module and HX in (A). The DCMD feed inlet temperature, initially at T_H, drops along the DCMD module due to evaporative cooling and conduction, reaching $T_C + \Delta T_{MD}$ at the feed outlet. The transmembrane vapor flux, ΔQ, is added to supplement the feed stream (at T_C) to maintain constant flow rate ratio, bringing the feed temperature down very slightly to T_{mix}. Before returning to the feed inlet, the feed passes the HX, where it increases in temperature to $T_H - \Delta T_{MD} - \Delta T_{HX}$, then the heat source, where it increases in temperature by $\Delta T'_{HS}$ or back to the working temperature, T_H. Here $\Delta T'_{HS}$, which is related to the power input into the system, is reduced due to the presence of the HX. The distillate loop temperature, initially at T_C, increases along the module due to vapor condensation and conduction, reaching $T_H - \Delta T_{MD}$ at the distillate outlet. The distillate then passes the HX, decreasing in temperature as the latent heat is used to preheat the feed stream, then the transmembrane vapor flux, ΔQ, is removed from the system to maintain constant flow rate ratio. Finally, the remaining distillate passes a heat sink where it reaches the operating temperature, T_C, and enters back into the DCMD module.

impact of salt concentration on $\bar{h}_{vap}$ is very small. The independence of SEC_{th} on salt concentration allows us to apply Eq. (10) for analyzing the energy consumption of the system even if the system is transient due to the feed solution being concentrated.

3.2. Specific energy consumption for a DCMD system with HX

The SEC_{th} can be significantly reduced by coupling an HX with a DCMD system to recover the latent heat of condensation (Fane et al., 1987). Specifically, the distillate stream in the DCMD module warms up by acquiring the heat transferred from the feed stream via both vapor transfer and conductive heat transfer. The heat that accumulates in the warm distillate effluent can be harvested to pre-heat the feed stream to a certain temperature to reduce the required power from the heat source to raise the influent feed stream temperature to T_H (Fig. 5).

If we again apply the assumption of negligible temperature change due to the blending of the supplementing feed water into the feed loop, then the temperature-rise of the feed stream flowing through the heat source is given by the follow equation according to the temperature profiles in Fig. 5B:

$$\Delta T_{HS}^{'} = \Delta T_{MD} + \Delta T_{HX} \tag{11}$$

where ΔT_{HX} is the temperature difference between the hot and cold streams in the HX. In this case, the specific energy consumption, SEC', can be quantified as

$$SEC'_{th} = \frac{P_{th}}{\Delta Q} = \frac{c_F Q_F \Delta T_{HS}{}'}{c_F Q_F (\Delta T - \Delta T_{MD})\eta_{th}/\bar{h}_{vap}} = \frac{\bar{h}_v}{\eta_{th}} \frac{\Delta T_{MD} + \Delta T_{HX}}{\Delta T - \Delta T_{MD}} \tag{12}$$

Here, the term $(\Delta T_{MD} + \Delta T_{HX})/(\Delta T - \Delta T_{MD})$ accounts for impact of the latent heat recovery. Eq. (12) suggests that SEC'_{th} can be reduced by reducing ΔT_{MD} and/or ΔT_{HX}. A smaller ΔT_{MD} indicates more heat from the influent feed stream (into the DCMD module) is transferred and stored in the effluent of the distillate stream, while a smaller ΔT_{HX} indicates a larger fraction of the heat stored in the distillate stream is recovered to heat up the feed stream in the HX. However, we note that, with the same feed and distillate stream flow rates, the achievement of smaller ΔT_{MD} and ΔT_{HX} requires larger MD membrane area and HX area, respectively, which consequently leads to lower vapor flux in the DCMD module and lower heat flux in the HX. This is a classic tradeoff between "kinetics and energy efficiency", (Lin and Elimelech, 2017; Wang and Lin, 2018) which is manifested in this case as a positive correlation between vapor/heat fluxes and SEC'. (Swaminathan et al., 2016)

Lastly, we note that the implementation of HX does not guarantee energy saving. Mathematically, this can be shown by the critical condition where SEC_{th} in Eq. (10) equals SEC'_{th} in Eq. (12):

$$\Delta T = 2\Delta T_{MD} + \Delta T_{HX} \tag{13}$$

With this critical condition, the same specific energy is consumed regardless of whether the HX is implemented or not. This critical condition corresponds to the scenario where the effluent temperature of the feed stream in the DCMD module, $T_C + \Delta T_{MD}$, is the same as the effluent temperature of the feed stream in the HX, $T_H - \Delta T_{MD} - \Delta T_{HX}$, so that heating up either stream using the external heat source requires the same amount of power. If the effluent temperature of the feed stream in the DCMD module is even higher than that in the HX, i.e., $\Delta T < 2\Delta T_{MD} + \Delta T_{HX}$, it would become more energy efficient to simply eliminate the HX and operate the system as in Fig. 4A, because the feed stream effluent in the DCMD module would not be able to receive any heat from a stream with even lower temperature. An extreme case of such a condition would be $\Delta T < 2\Delta T_{MD}$, which suggests that the effluent of the feed stream is even warmer than the effluent of the distillate stream in the DCMD module and thus no latent heat can possibly be recovered. This usually occurs when there is insufficient membrane area to recover enough feed water, which leads to poor single-pass water recovery (as compared to the thermodynamic limit) but relatively high vapor flux due to the conservation of driving force (i.e., transmembrane temperature difference). The very extreme case for such a scenario is when a small membrane coupon is used instead of membrane module: due to the insufficient residence time of the feed and distillate streams, very little water is recovered and the temperatures of the feed and distillate streams also experience negligible change.

3.3. Gained output ratio

In thermal desalination processes, the gained output ratio, or GOR, is often used as a metric to quantify the energy efficiency. GOR is defined as the mass of distillate produced per mass of vapor generated, which in effect quantifies the "number of times" latent heat of condensation is reused. Therefore, GOR is mathematically the ratio between the latent heat and the specific energy consumption. Its non-dimensionality and the use of latent heat as reference make it an informative alternative to specific energy consumption for quantifying the energy efficiency of an MD process. For DCMD without HX, GOR is simply η_{th}. When HX is employed, GOR can be described as

$$GOR \approx \eta_{th} \frac{\Delta T - \Delta T_{MD}}{\Delta T_{MD} + \Delta T_{HX}} \tag{14}$$

Eq. (14) clearly suggests that GOR depends on four parameters, η_{th}, ΔT, ΔT_{MD} and ΔT_{HX}. If we assume that $\Delta T_{MD} = \Delta T_{HX}$, which is practically unnecessary but would nonetheless simplify our analysis, we can illustrate the results from Eq. (14) using Fig. 6. GOR can be improved by (1) improving η_{th}, (2) reducing ΔT_{MD} and ΔT_{HX}, and (3) using a larger ΔT which is equivalent to using a higher influent feed temperature T_H if we assume T_C to be fixed. With a ΔT of 60 °C (e.g., T_H= 80 °C and T_C = 20 °C), a ΔT_{MD} and a ΔT_{HX} of 5 °C (practical minima), and a thermal efficiency, η_{th}, of 80% (in the high practical range), the corresponding GOR according to Eq. (14) is 4.4. Based on such an analysis, it is practically challenging to push the GOR beyond five. If a GOR of 5 can indeed be achieved, the ΔT_{MD} and ΔT_{HX} must be so small that vapor flux for the MD process and heat flux in the HX are both impractically low.

4. Energy efficiency analysis for MD powered by waste heat streams

While waste heat may exist in different forms, one major source of waste heat is hot streams from power generation and industrial processes. The major difference of hot streams from a conceptual constant temperature heat source as defined earlier is the change of stream

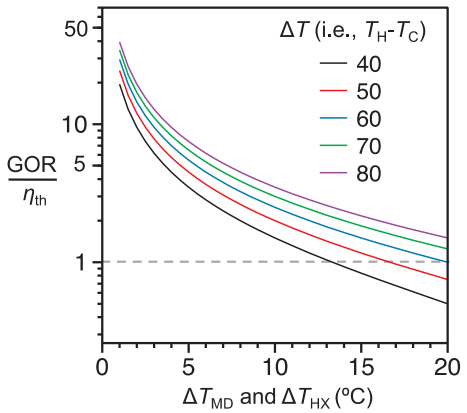

Fig. 6. Gained output ratio (GOR) over thermal efficiency (η_{th}) plotted as a function of transmembrane temperature difference (ΔT_{MD}) and the temperature difference between the hot and cold streams along the HX (ΔT_{HX}) according to **Eq. (14)**. ΔT_{MD} and ΔT_{HX} were assumed to be constant for ease of analysis. A series of six ΔT values, or the difference between the DCMD feed inlet (T_H) and the distillate inlet (T_C), relevant to MD were included in the analysis.

temperature as a hot stream gives away heat. The schematics of DCMD system powered by an external hot stream as the heat source and the corresponding temperature profiles in different components are presented in Fig. 7 and Fig. 8 for two system designs, one with HX and the other without. The heat source is essentially an additional HX exchanging heat between the feed stream and waste heat stream. We refer to this additional HX as HX_2 in the following discussion. A DCMD system always requires an HX_2 for extracting heat from the waste heat stream, whereas HX_1 is for recovering the latent heat stored in the warm distillate effluent and is thus optional.

For DCMD without an HX for recovering the accumulated heat in the distillate, the cool effluent of the feed channel in the MD module blends with the supplementary feed stream and then enters the HX_2 to absorb heat from the waste-heat stream (ws) (Fig. 7A). The temperature of WS decreases from the influent (i) temperature, $T_{ws,i}$, to the effluent (e) temperature $T_{ws,e}$ due to the release of heat to the feed stream (Fig. 7B). To describe the behavior of HX_2, we denote the temperature difference of the two exchanging streams at the exit of the waste-heat stream (i.e., the entrance of the cold stream in HX_2) as ΔT_{HX2}. We note that (1) this temperature difference is dependent on the flow rates of the two stream and the available area for heat transfer in the HX; and (2) unlike in the DCMD module or HX_1 where the flows of heat capacity for the two streams are similar when operation is optimized, there is no required relationship between the flow rates of the two streams in HX_2. Therefore, ΔT_{HX2} is only defined at the exit of the waste-heat stream and does not necessarily apply to other position in HX_2. The effluent temperature of waste-heat stream, after surrendering the power of P_{th}, is

$$T_{ws,e} = T_H - \Delta T_{HS} + \Delta T_{HX2} = T_C + \Delta T_{MD} + \Delta T_{HX2} \quad (15)$$

When a waste-heat stream is used as the heat source for the DMCD system equipped with an HX for heat recovery, the system is designed following the schematic shown in Fig. 8A. Accordingly, the temperature profiles in the MD module and in HX (for heat recovery) and HX_2 (as the heat source) are shown in Fig. 8B. In this case, the effluent temperature of waste-heat stream, after surrendering the power of P_{th}, is

$$T'_{ws,e} = T_H - \Delta T'_{HS} + \Delta T_{HX2} = T_H - \Delta T_{MD} - \Delta T_{HX} + \Delta T_{HX2} \quad (16)$$

4.1. Gained output ratio when waste-heat stream is used as the heat source

While the system schematics and the temperature distribution profiles appear to be more complicated when a waste-heat stream replaces a constant-temperature heat source, the way to calculate SEC_{th} and GOR, are no different from those as described in Section 3. This is because, the analysis in Section 3 only assumes that a certain power is extracted from the heat source but does not specify the working mechanism of the heat source. Therefore, whether the heat source is a constant-temperature heat source or a waste-heat stream does not affect the calculation and results of the SEC_{th} and GOR. Based on these metrics of energy efficiency, installing an HX for recovering the heat accumulated in the distillate effluent stream, as depicted in Fig. 7A, is of paramount importance even if a waste-heat stream is used as the heat source. However, comparing Fig. 7B and Fig. 8B suggests that, because of the different power extracted from the waste-heat stream, the effluent temperatures of the waste-heat streams also differ depending on whether heat recovery from distillate stream is implemented. A lower effluent temperature of the waste-heat stream suggests that a larger fraction of the available waste-heat is utilized. This is another piece of important information that is not reflected by conventional metrics for energy efficiency, such as SEC_{th} and GOR.

4.2. Specific yield and waste-heat utilization efficiency

When waste-heat streams are used as the heat source, we propose an alternative metric to describe "energy efficiency", namely the specific yield (SY). SY is defined as the ratio between the *trans*-membrane vapor flow rate and the power of the "available heat," $P_{th,ws,max}$, which can be quantified as

$$P_{th,ws,max} = c_{ws} Q_{ws} (T_{ws,i} - T_C) \quad (17)$$

where c_{ws} and Q_{ws} are the specific heat capacity and the flow rate of the waste-heat stream. The difference between $T_{ws,i}$ and T_C determines $P_{th,ws,max}$ because the waste-heat stream theoretically would not be able to provide any more heat to the feed stream once its temperature approaches T_C (i.e., there will not be any driving force). Because c_{ws} and Q_{ws} are independent of any property in the MD system, for any given waste-heat stream we can treat $P_{th,ws,max}$ as a constant that is independent of the design (e.g., whether to include heat recovery or not) and operation of the MD system. Based on the definition of SY and Eq. (9):

$$SY = \frac{\Delta Q}{P_{th,ws,max}} = \frac{c_F Q_F (\Delta T - \Delta T_{MD}) \eta_{th}}{\bar{h}_{vap} P_{th,ws,max}} \quad (18)$$

Eq. (18) suggests that SY is roughly fixed as long as feed stream

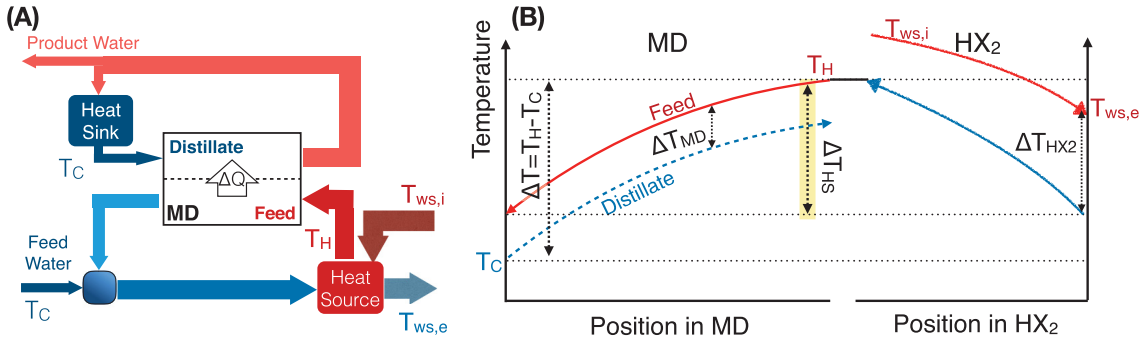

Fig. 7. (A) Countercurrent DCMD system with recycled feed and distillate streams and an HX (HX_2) to recover heat from a waste-heat stream (ws) as the heat source. The heat source is required to maintain the working temperature (T_H) and a heat sink is required to maintain the distillate inlet temperature (T_C). (B) Temperature profiles of the feed and distillate streams along the DCMD module and HX_2 in (A). The DCMD feed inlet temperature, initially at T_H, drops along the DCMD module due to evaporative cooling and conduction, reaching $T_C + \Delta T_{MD}$ at the feed outlet. The transmembrane vapor flux, ΔQ, is added to supplement the feed stream (at T_C) to maintain constant flow rate ratio, bringing the feed temperature down very slightly to T_{mix}. Before returning to the feed inlet, the feed passes HX_2 where it increases in temperature by ΔT_{HS} back to the working temperature. Here ΔT_{HX2} is the temperature difference at the outlet of both streams in HX_2. The temperature difference along HX_2 is not important to this analysis as we are only concerned with the total power delivered from the heat source. The waste-heat stream decreases in temperature from the inlet ($T_{ws,i}$) to the effluent ($T_{ws,e}$) as heat transfers into the feed stream, bringing it back to the working temperature. The distillate loop temperature, initially at T_C, increases along the module due to vapor condensation and conduction, reaching $T_H - \Delta T_{MD}$ at the distillate outlet. The transmembrane vapor flux, ΔQ, is removed from the system distillate to maintain constant flow rate ratio. The remaining distillate passes a heat sink where it reaches the operating temperature, T_C, and enters back into the DCMD module.

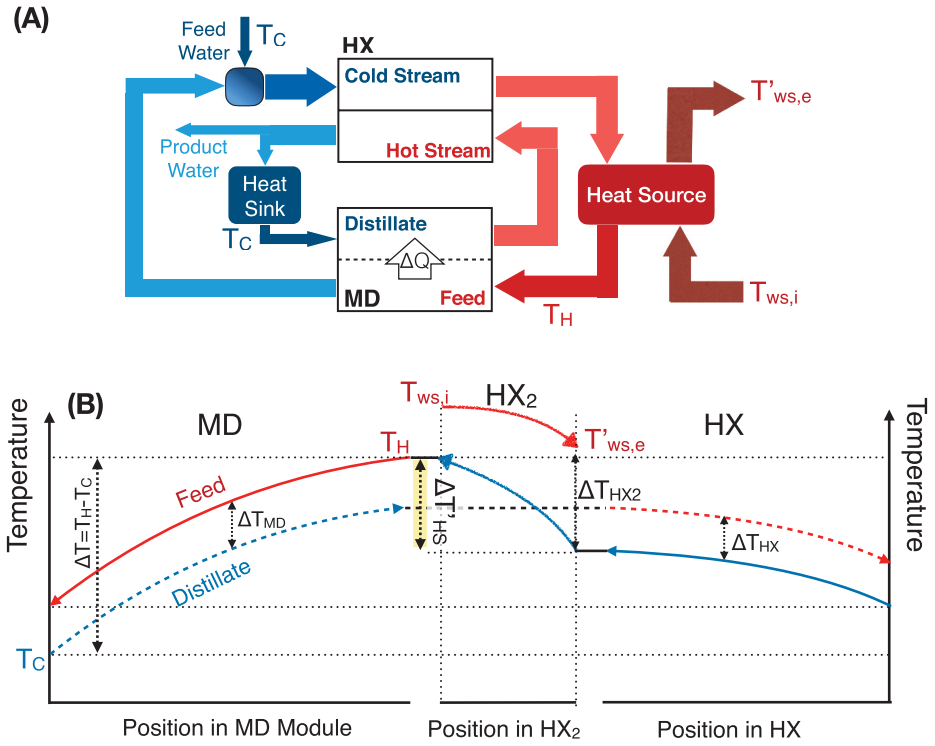

Fig. 8. (A) Countercurrent DCMD system with recycled feed and distillate streams and HX_1 to recover heat from the distillate stream and HX_2 to harness heat from a waste-heat stream (ws) as a heat source. The heat source is required to maintain the working temperature (T_H) and a heat sink is required to maintain the distillate inlet temperature (T_C). (B) Temperature profiles of the feed and distillate streams along the DCMD module, HX_1, and HX_2 in (A). The DCMD feed inlet temperature, initially at T_H, drops along the MD module due to evaporative cooling and conduction, reaching $T_C + \Delta T_{MD}$ at the feed outlet. The transmembrane vapor flux, ΔQ, is added to supplement the feed stream (at T_C) to maintain constant flow rate ratio, bringing the feed temperature down very slightly to T_{mix}. The feed then passes HX_1, where it increases in temperature to $\Delta T_H - \Delta T_{HS}$. Here ΔT_{HS} is the heat that must be supplied by the heat source, HX_2. The feed then passes HX_2 where it is brought back to the working temperature. Here ΔT_{HX2} is the temperature difference at the outlet of both streams in HX_2. The temperature difference along HX_2 is not important to this analysis as we are only concerned with the total power delivered from the heat source. The waste-heat stream decreases in temperature from the inlet ($T_{ws,i}$) to the effluent ($T'_{ws,e}$) as heat transfers into the feed stream, bringing it back to the working temperature. The distillate loop temperature, initially at T_C, increases along the module due to vapor condensation and conduction, reaching $T_H - \Delta T_{MD}$ at the distillate outlet. The distillate then passes HX_1 where it decreases in temperature to $T_C + \Delta T_{MD} + \Delta T_{HX}$. The transmembrane vapor flux, ΔQ, is removed from the system distillate to maintain constant flow rate ratio and the remaining distillate passes a heat sink to bring it to the operating temperature, T_C, where it re-enters the DCMD module.

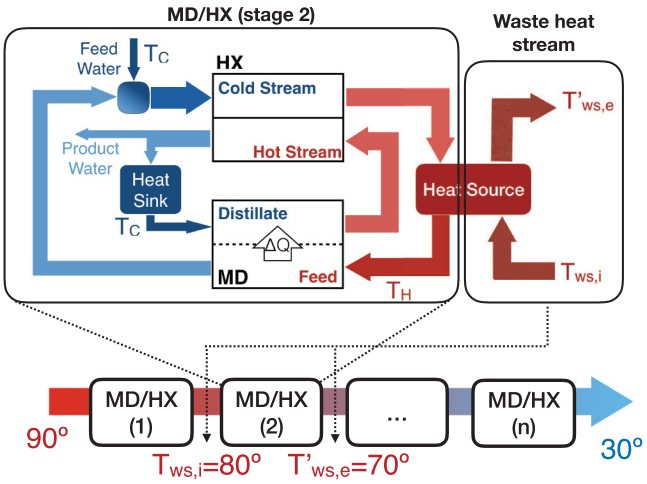

Fig. 9. Multiple stages of DCMD module integrated with an HX to recover latent heat from its distillate stream. The heat implemented into the system to maintain the working temperature is transferred via heat exchanger (HX_2) from a waste-heat stream. Including multiple MD/HX stages increases the waste-heat usage efficiency. Each individual stage consists of the system analyzed in Fig. 8.

properties (e.g. c_F and Q_F) and operating conditions (e.g. ΔT and ΔT_{MD}) are maintained constant. In other words, for a given waste-heat stream with a certain power, how much water can be generated in a unit time is only dependent on how the DCMD process is operated but not on whether latent heat recovery is implemented.

To further elucidate this point, we define waste-heat utilization efficiency, η_{ws}, as the ratio between the power of the heat absorbed by the MD system for water production, P_{th}, and the power of the available heat, $P_{th,ws,max}$. We note that η_{ws} is essentially the *effectiveness* of HX_2, defined as the ratio between the actual heat transfer rate and the maximum possible heat transfer rate (Swaminathan et al., 2016). According to such a definition, η_{ws}, can be expressed as

$$\eta_{ws} = \frac{P_{th}}{P_{th,ws,max}} = \frac{T_{ws,i} - T_{ws,e}(or T'_{ws,e})}{T_{ws,i} - T_C} \tag{19}$$

Here, $T_{ws,e}$ as in Eq. (19) is used when latent heat recovery is not implemented, whereas $T'_{ws,e}$ is used when an HX is integrated to recover the latent heat accumulated in the distillate effluent stream. Given the same waste-heat stream (i.e., the same c_{ws}, Q_{ws}, and $T_{ws,i}$), $T'_{ws,e}$ is always higher than $T_{ws,e}$, and η_{ws} is thus lower when latent heat recovery is implemented. The relationship between η_{ws}, SEC_{th}, and SY can be more clearly illustrated using the following expression derived by combining Eq. (18) and the definition of SEC_{th}:

$$SY = \frac{\eta_{ws}}{SEC_{th}} \tag{20}$$

We note that Eqs. (19) and (20) are valid if we consider a liquid waste heat stream (e.g., a stream of hot water) that would not undergo phase change, which will be the focus of this analysis for its simplicity.

However, if a low pressure/temperature steam is used as the waste heat stream, then the apparent heat due to the temperature change of the stream in both vapor and liquid phase and latent heat due to phase change must be all considered.

Because we have shown that SY is independent of the presence or the degree of latent heat recovery, Eq. (20) simply suggests that the ratio between η_{ws} and SEC_{th} is constant. The constant η_{ws}/SEC can be interpreted as following: when latent heat recovery is implemented, the MD process as a whole is more energy efficient with a lower SEC_{th} (except when $\Delta T < 2\Delta T_{MD} + \Delta T_{HX}$), but at the same time, a smaller fraction of the available waste-heat is utilized to drive the MD process (i.e., $\eta_{ws}$is smaller); in contrast, when latent recovery is not implemented, the MD process is less energy efficient as indicated by a higher SEC_{th}, but a larger fraction of the available waste-heat is utilized. It therefore does not matter whether latent heat recovery is implemented, or to what extent is implemented, if the performance metric chosen to assess the system is SY.

4.3. Improving specific yield with multiple stages

Following the above discussion, substantial enhancement of SY must involve improving η_{ws} and SEC_{th} simultaneously. This can be achieved by implementing multi-stage DCMD with each stage integrating an HX for heat recovery (Fig. 9). Here, each stage is essentially an independent DCMD system absorbing heat from the waste-heat stream at a certain temperature range. We note that the definition of a multi-stage system here is different from the multi-stage or multi-effect vacuum MD or air-gap MD where the multiple stages or effects are implemented to maximize latent heat recovery. The multiple stages in Fig. 9 are implemented to maximize the utilization of the thermal energy in the waste-heat stream. In the case when n stages are implemented, the specific yield, SY is given by the following expression:

$$SY = \sum_{k=1}^{n} \frac{\eta_{ws,k}}{SEC_{th,k}} \tag{21}$$

where $\eta_{ws,k}$ and $SEC_{th,k}$ are the waste-heat utilization efficiency (defined by Eq. (19)) and the specific energy consumption (defined by Eq. (12)) for the k stage, respectively.

Implementing more stages will certainly enhance the overall specific yield, but it requires substantially more capital investment. Due to the dependence of SEC_{th} on ΔT, the SEC_{th} of later stages is higher if ΔT_{MD} and ΔT_{HX} are maintained the same (Eq. (12)), i.e., the MD/HX systems are less efficient in later stages. We also expect the vapor flux to be substantially lower in later stages as the partial vapor pressure difference corresponding to the same ΔT_{MD} is significantly smaller when the average of the feed and the distillate stream temperatures is lower (Wang and Lin, 2018; Sandler, 2006). Both the considerations of SEC and vapor flux suggest a diminishing return for installing additional stages in the lower temperature range. Therefore, whether or not multiple stages should be implemented and how many stages should be implemented are strongly dependent on the relative economic value of the product water as compared to the capital cost.

5. Conclusion and implications

In this study we first highlight the importance of balancing heat capacity flows between the feed and distillate streams in MD for optimal performance. We discuss the presence of two operating regimes, the distillate limiting regime (DLR) and the feed limiting regime (FLR), as demarcated by α^*, the critical flow rate ratio. The novelty of this work is the development of an approximation for the critical flow rate ratio that eases the understanding of module-scale MD energy analysis and optimization. We also define an approximation for the maximum single pass water recovery, R_{max}, for the two regimes based on a simple energy balance over the vapor. While some of these concepts have been derived in previous study, here we re-derive them using more intuitive and comprehensible principles and showed the approximation is both simple and accurate when compared to a precise numerical solution derived in previous work.

We also provide a framework for evaluating the energy efficiency of MD in two configurations, with and without an integrated heat exchanger (HX) to recover latent heat from the distillate stream. Our analysis reveals the presence of a critical condition to determine if the implementation of HX results to energy saving. Because MD is attractive for its ability to use low grade waste heat, for the first time we present a framework for analyzing energy efficiency of MD powered by waste heat stream. We define a new metric, specific yield, which quantifies the performance of MD powered by waste heat stream. For a single-stage MD powered by a waste heat stream, whether implementing latent heat recovery or not only affects the SEC_{th} (or GOR) of the process, but not the specific yield. In other words, although implementing latent heat recovery for a single-stage MD deriving heat from a waste heat stream appears to improve the efficiency in the conventional metrics such as SEC_{th} and GOR, it does not actually better utilize the available waste heat for desalination. Multi-stage MD with latent heat recovery can more efficiently harness the available waste heat, but its economics may be questionable and require further investigation.

The approximations derived in this work are not only satisfactorily accurate, but can be calculated from easily measurable quantities. The presented framework for energy efficiency analysis in MD does not involve computationally heavier heat and mass transfer simulations, Consequently, this framework will be useful for high-level techno-economic evaluation and module-scale optimization, which is strongly relevant for practical application of MD in industry.

CRediT authorship contribution statement

Kofi S.S. Christie: Formal analysis, Writing - original draft. **Thomas Horseman:** Formal analysis, Writing - original draft. **Shihong Lin:** Conceptualization, Formal analysis, Writing - original draft, Writing - review & editing, Supervision, Funding acquisition.

Declaration of Competing Interest

The authors declare that they have no known competing financial interests or personal relationships that could have appeared to influence the work reported in this paper.

Acknowledgement

This work is supported by US National Science Foundation Grant CBET-1739884. K.S.S.C. also acknowledges the support from US National Science Foundation via an NSF-GRFP award DGE-1145194.

Appendix A. Supplementary material

Supplementary data to this article can be found online at https://doi.org/10.1016/j.envint.2020.105588.

References

Alkhudhiri, A., Darwish, N., Hilal, N., 2012. Membrane distillation: a comprehensive review. Desalination 287, 2–18.
Alklaibi, A.M., Lior, N., 2006. Heat and mass transfer resistance analysis of membrane distillation. J. Memb. Sci. 282, 362–369.
Bergman, T.L., Lavine, A.S., Incropera, F.P., Dewitt, D.P., 2011. Fundamentals of heat and mass transfer. John Wiley & Sons Inc.
Bui, V.A., Vu, L.T.T., Nguyen, M.H., 2010. Modelling the simultaneous heat and mass transfer of direct contact membrane distillation in hollow fibre modules. J. Memb. Sci. 353, 85–93.
Camacho, L.M., et al., 2013. Advances in membrane distillation for water desalination and purification applications. Water (Switzerland) 5, 94–196.
Cath, T.Y., Adams, V.D., Childress, A.E., 2004. Experimental study of desalination using

direct contact membrane distillation: a new approach to flux enhancement. J. Memb. Sci. 228, 5–16.
Cheng, L.H., Wu, P.C., Chen, J., 2008. Modeling and optimization of hollow fiber DCMD module for desalination. J. Memb. Sci. 318, 154–166.
Chung, S., Seo, C.D., Lee, H., Choi, J.H., Chung, J., 2014. Design strategy for networking membrane module and heat exchanger for direct contact membrane distillation process in seawater desalination. Desalination 349, 126–135.
Creusen, R., et al., 2013. Integrated membrane distillation-crystallization: Process design and cost estimations for seawater treatment and fluxes of single salt solutions. Desalination 323, 8–16.
Curcio, E., Drioli, E., 2005. Membrane distillation and related operations - A review. Sep. Purif. Rev. 34, 35–86.
Deshmukh, A., et al., 2018. Membrane distillation at the water-energy nexus: Limits, opportunities, and challenges. Energy Environ. Sci. 11, 1177–1196.
Drioli, E., Ali, A., Macedonio, F., 2015. Membrane distillation: Recent developments and perspectives. Desalination 356, 56–84.
Fane, A.G., Schofield, R.W., Fell, C.J.D., 1987. The efficient use of energy in membrane distillation. Desalination 64, 231–243.
González-Bravo, R., Elsayed, N.A., Ponce-Ortega, J.M., Nápoles-Rivera, F., El-Halwagi, M.M., 2015. Optimal design of thermal membrane distillation systems with heat integration with process plants. Appl. Therm. Eng. 75, 154–166.
Gryta, M., Tomaszewska, M., 1998. Heat transport in the membrane distillation process. J. Memb. Sci. 144, 211–222.
Guan, G., Yang, X., Wang, R., Fane, A.G., 2015. Evaluation of heat utilization in membrane distillation desalination system integrated with heat recovery. Desalination 366, 80–93.
Gustafson, R.D., Hiibel, S.R., Childress, A.E., 2018. Membrane distillation driven by intermittent and variable-temperature waste heat: System arrangements for water production and heat storage. Desalination 448, 49–59.
Hausmann, A., Sanciolo, P., Vasiljevic, T., Weeks, M., Duke, M., 2012. Integration of membrane distillation into heat paths of industrial processes. Chem. Eng. J. 211–212, 378–387.
Kim, Y.D., Thu, K., Choi, S.H., 2015. Solar-assisted multi-stage vacuum membrane distillation system with heat recovery unit. Desalination 367, 161–171.
Lee, H., He, F., Song, L., Gilron, J., Sirkar, K.K., 2011. Desalination with a Cascade of Cross-Flow Hollow Fiber Membrane Distillation Devices Integrated with a Heat Exchanger. Am. Inst. Chem. Eng. J. 57, 1780–1795.
Lin, S., Elimelech, M., 2017. Kinetics and energetics trade-off in reverse osmosis desalination with different configurations. Desalination 401, 42–52.
Lin, S., Yip, N.Y., Elimelech, M., 2014. Direct contact membrane distillation with heat recovery: thermodynamic insights from module scale modeling. J. Memb. Sci. 453, 498–515.
Lu, Y., Chen, J., 2012. Integration design of heat exchanger networks into membrane distillation systems to save energy. Ind. Eng. Chem. Res. 51, 6798–6810.
Maheswari, K.S., Kalidasa Murugavel, K., Esakkimuthu, G., 2015. Thermal desalination using diesel engine exhaust waste heat - an experimental analysis. Desalination 358, 94–100.
Martínez-Díez, L., Vázquez-González, M.I., 2000. A method to evaluate coefficients affecting flux in membrane distillation. J. Memb. Sci. 173, 225–234.
Martínez-Díez, L., Vázquez-González, M.I., Florido-Díaz, F.J., 1998. Study of membrane distillation using channel spacers. J. Memb. Sci. 144, 45–56.
Phattaranawik, J., Jiraratananon, R., Fane, A.G., Halim, C., 2001. Mass flux enhancement using spacer filled channels in direct contact membrane distillation. J. Memb. Sci. 187, 193–201.
Phattaranawik, J., Jiraratananon, R., 2001. Direct contact membrane distillation: effect of mass transfer on heat transfer. J. Memb. Sci. 188, 137–143.
Phattaranawik, J., Jiraratananon, R., Fane, A.G., 2003. Heat transport and membrane distillation coefficients in direct contact membrane distillation. J. Memb. Sci. 212, 177–193.
Qtaishat, M., Matsuura, T., Kruczek, B., Khayet, M., 2008. Heat and mass transfer analysis in direct contact membrane distillation. Desalination 219, 272–292.
Sandler, S.I., 2006. Chemical, Biochemical, and Engineering Thermodynamics. John Wiley & Sons Inc.
Schofield, R.W., Fane, A.G., Fell, C.J.D., 1987. Heat and mass transfer in membrane distillation. J. Memb. Sci. 33, 299–313.
Semblante, G.U., Lee, J.Z., Lee, L.Y., Ong, S.L., Ng, H.Y., 2018. Brine pre-treatment technologies for zero liquid discharge systems. Desalination 441, 96–111.
Shaffer, D.L., et al., 2013. Desalination and reuse of high-salinity shale gas produced water: Drivers, technologies, and future directions. Environ. Sci. Technol. 47, 9569–9583.
Shannon, M.A., et al., 2009. Science and technology for water purification in the coming decades. Nanosci. Technol. A Collect. Rev. from Nat. Journals 452, 337–346.
Song, L., Li, B., Sirkar, K.K., Gilron, J.L., 2007. Direct contact membrane distillation-based desalination: novel membranes, devices, larger-scale studies, and a model. Ind. Eng. Chem. Res. 46, 2307–2323.
Summers, E.K., Arafat, H.A., Lienhard, V.J.H., 2012. Energy efficiency comparison of single-stage membrane distillation (MD) desalination cycles in different configurations. Desalination 290, 54–66.
Swaminathan, J., et al., 2016. Energy efficiency of permeate gap and novel conductive gap membrane distillation. J. Memb. Sci. 502, 171–178.
Swaminathan, J., Chung, H.W., Warsinger, D.M., Lienhard, V.J.H., 2016. Membrane distillation model based on heat exchanger theory and configuration comparison. Appl. Energy 184, 491–505.
Swaminathan, J., Chung, H.W., Warsinger, D.M., Lienhard, J.H., 2016. Simple method for balancing direct contact membrane distillation. Desalination 383, 53–59.
Swaminathan, J., Chung, H.W., Warsinger, D.M., 2018. Energy efficiency of membrane distillation up to high salinity: Evaluating critical system size and optimal membrane thickness. Appl. Energy 211, 715–734.
Termpiyakul, P., Jiraratananon, R., Srisurichan, S., 2005. Heat and mass transfer characteristics of a direct contact membrane distillation process for desalination. Desalination 177, 133–141.
Tong, T., Elimelech, M., 2016. The global rise of zero liquid discharge for wastewater management: drivers, technologies, and future directions. Environ. Sci. Technol. 50, 6846–6855.
Wang, L., Lin, S., 2018. Intrinsic tradeoff between kinetic and energetic efficiencies in membrane capacitive deionization. Water Res. 129, 394–401.
Warsinger, D.M., Mistry, K.H., Nayar, K.G., Chung, H.W., Lienhard, J.H.V., 2015. Entropy generation of desalination powered by variable temperature waste heat. Entropy 17, 7530–7566.
Zuo, G., Wang, R., Field, R., Fane, A.G., 2011. Energy efficiency evaluation and economic analyses of direct contact membrane distillation system using Aspen Plus. Desalination 283, 237–244.